

Microfluidic mixers: from microfabricated to self-assembling devices

BY CHRISTOPHER J. CAMPBELL AND BARTOSZ A. GRZYBOWSKI

*Department of Chemical and Biological Engineering, Northwestern University,
2145 Sheridan Rd, Evanston, 60208 IL, USA (grzybor@northwestern.edu)*

Published online 16 March 2004

This paper begins with a survey of both passive and active microfluidic mixers that have been implemented in recent years. It then describes a micromixing device based on dynamic self-assembly. This device is easy to fabricate and has excellent working characteristics in the continuous-flow mode. The paper concludes with a brief discussion of possible applications of self-assembly in microfluidics.

Keywords: microfluidics; mixing; micromixers; self-assembly

1. Introduction

Mixing (Chaté *et al.* 1999; Ottino 1988) is not only a ubiquitous natural phenomenon accompanying geophysical, ocean and atmospheric flows (Plumb 1993), but it is also an important step in many technological processes. Effective mixing underlies the operation of chemical (Fogler 1999) and fermentation (Blakebrough 1967) reactors, combustion engines (Kuo 1986) and other processes (Radovanovic 1986); it is required to make glasses (Tooley 1984; West 1984), polymer blends (Charrier 1991) and pharmaceutical formulations (Walsh 1998). The majority of these industrial processes are carried out on macroscopic scales (kilogrammes to tonnes), and it has only been in the recent years that mixing of small quantities of liquids has become technologically relevant in the context of microfluidics (Tay 2002; Nguyen & Werely 2002) and micro total analysis systems (μ TAS) (Auroux *et al.* 2002; Knight 2002; Legge 2001; Reyes *et al.* 2002).

Mixing on microscopic scales is, however, difficult. Although diffusion on the microscale is fast (characteristic diffusion times scale with the square of the characteristic dimension), the Reynolds numbers are usually low ($Re \sim O(1)$), and the flows are laminar. In the absence of turbulence, it is hard to increase the interfacial area of contact through which the molecules diffuse.

Numerous and often ingenious micromixing devices have been developed that overcome the limitations imposed by the laminarity of microflows. Before discussing the architectures and principles of these micromixers in detail, a few words are in order to clarify certain nomenclatural nuances. Thus, both the process of mixing itself and the mixing devices are classified as either passive or active—these terms, however, have very different meanings in each of the contexts. Specifically, passive mixing

One contribution of 11 to a Theme ‘Transport and mixing at the microscale’.

refers to processes in which the interfaces between the substances being mixed follow the flow and have no back-effect on it, while active mixing refers to processes in which the interfaces interact with the flow and modify it (Ottino 1988). Passive mixers, on the other hand, are those that have no moving parts and achieve mixing by virtue of their topology alone, while active mixers either do have moving parts or they use externally applied forcing functions such as pressure or electromagnetic fields (Evans *et al.* 1997; Lee *et al.* 2000; Oddy *et al.* 2001). In principle, one can have active mixing in a passive mixer or vice versa. To avoid any confusion, we will use the terms ‘passive’ and ‘active’ only as they are habitually used in the context of mixing devices.

Passive mixers use the channel geometry to either laminate the flowing fluids in-plane or out-of-plane to promote chaotic advection in these fluids. Both approaches lead to an increase in the interfacial area and, consequently, to better mixing; some commonly used architectures of passive mixers are summarized in table 1. Although the lack of moving parts makes passive mixers free of additional friction and wear effects, their intricate channel topologies are often hard to microfabricate, and they are generally not switchable: once incorporated in a fluidic system, they perform their function whenever fluids pass through them. In contrast, active mixers can be controlled externally, which makes them suitable components of reconfigurable microfluidic systems: that is, systems that can perform several different functions given different states of external controls. The advantage of controllability is somewhat offset by the complicated microfabrication that is often needed to make active mixing microdevices.

Below we will discuss various approaches to active mixers (AMs) in detail. We will start with a brief discussion of (i) what effective mixing is and (ii) what types of physical phenomena/effects can, at least in principle, be used to actively mix microscopic amounts of fluids. We will then review which of these phenomena have been used in reported active mixers: we will describe how these mixers were fabricated; what phenomena underlie their operation; how efficiently they function; and what their major limitations are. Next, we will present a new approach to active micromixing that is based on dynamic self-assembly (DySA) (Grzybowski *et al.* 2000, 2002; Grzybowski & Whitesides 2002*a, b*; Whitesides & Grzybowski 2002) and that circumvents most of the microfabrication problems encountered in ‘conventional’ active mixers. We will conclude with a discussion of the possible uses of self-assembly in the development of other types of AM and of entire microfluidic systems.

2. Efficient micromixing

The efficiency of mixing between two fluids is directly related to the area of an interface between them through which molecular diffusion can occur; the greater this area, the better the mixing. In macroscopic flows characterized by large Reynolds numbers ($Re \gtrsim 10^4$), mixing is facilitated by turbulence, which creates flow structures, and thus interfaces, on many different length-scales. ‘On the microscale, it is technically difficult to achieve turbulence in straight microchannels, where the onset of turbulence occurs at $Re > 2000$, corresponding to a flow rate of 20 m s^{-1} in a channel $100 \text{ }\mu\text{m}$ wide. Although in rotary micromixers the onset of turbulence occurs at slightly lower Re values—on the order of a few hundred—it requires rotational

speeds that are still rather high. For example, a 0.5 mm rotary mixer would have to rotate with $\omega = 125$ Hz to reach $Re \sim 100$.’

There exists, however, another mechanism that gives rise to efficient mixing in the regime of low Reynolds numbers. The underlying idea of this so-called Lagrangian chaos (or ‘chaotic advection’) is the observation that certain regular and ‘smooth’ velocity fields can produce fluidic pathlines that uniformly fill the volume in an ergodic way. In such velocity fields, fluid elements that are originally close to one another trace paths that diverge rapidly (exponentially fast in the ideal case), so that the material is dispersed throughout the volume very efficiently. In the context of this paper, it is important to note that chaotic advection cannot occur in steady two-dimensional flows, but only in two-dimensional time-dependent and three-dimensional flows. From this theorem, we can immediately conclude that, for example, a small cylindrical rotor spinning around its centre with uniform angular frequency (Couette flow) is not likely to be an efficient micromixer, while two such rotors turned on and off at alternating times (the blinking vortex model) (Aref 1984) can form the basis of a useful microdevice. In very pictorial terms, good micromixing requires repeated stretching and folding of fluid elements. In Couette flow, the fluid is only stretched and the mixing is poor; in the arrangement of two alternating rotors, the fluid is repeatedly stretched around one of them and then folded around the other—hence, the mixing is good.

3. Active micromixers






Active micromixers (μ Mixers) can be classified according to whether or not they have moving parts. In micromixers with moving elements, these elements—be they microscopic stirrer bars, piezoelectric membranes or gas bubbles—can either rotate or they can perform oscillatory motions. Table 2 applies this classification to the μ Mixers that have been demonstrated to date; it also suggests two physical phenomena—electrorotation and magnetic actuation of magnetic droplets—that have not been used in actual designs but which we believe can be the basis of efficient mixers.

In the remaining part of this section, we describe principles of operation, designs and microfabrication of micromixers representative to each of the listed subcategories.

(a) Rotary motion

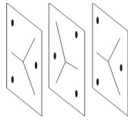
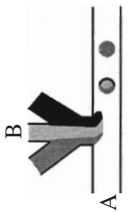
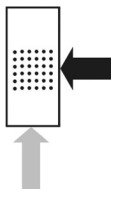

A rotary device has been developed with a 3×3 array of magnetic microstirrers, (each *ca.* 400 μ m long) powered by an external, rotating magnetic field (Lu *et al.* 2002). Each microstirrer consisted of a rotor attached to a hub, and was patterned from copper, chromium and gold layers supported on a glass wafer. The rotor was etched out of copper, and the hub out of chromium and gold. Once the rotors were made, a slab of poly(dimethyl siloxane) (PDMS) containing the fluidic network was registered and sealed against a glass slide supporting the mixers. In total, nine microfabrication steps were required to make the device. For a rotational speed of the rotors of $\omega = 600$ RPM, the device achieved complete mixing of a 10 μ l mixing volume within 55 s from the onset of stirring.

Table 1. *Examples of passive microfluidic mixers*
(Inlet fluids are marked in light grey and black.)

principle/phenomenon	typical architecture	volumes	times	mFAB	references
in-plane flow splitting		100 pL	<1 s	easy	He <i>et al.</i> (2001)
hydrodynamic focusing		5 nL	10 μ s	easy	Knight <i>et al.</i> (1998)
caterpillar flow splitting and recombination		100 nL	10 ms	hard	Ehrfeld <i>et al.</i> (2000a)
Möbius mixer: flow twisting		100 nL	10 ms	relatively hard	Ehrfeld <i>et al.</i> (2000b)
mixing by chaotic advection ^a		200 nL	1 s	relatively easy	Stroock <i>et al.</i> (2002)

^aChaotic advection is induced by chevron ridges embossed on the bottom of the channel.

Table 1. (*Cont.*)
(Inlet fluids are marked in light grey and black.)

principle/phenomenon	typical architecture	volumes	times	mFAB	references
multilamination through a stack of sheets ^b		40 $\mu\text{l s}^{-1}$	10 ms	hard	Ehrfeld <i>et al.</i> (2000b)
multilamination through a stack of sheets ^c		7.5 $\mu\text{l min}^{-1}$	2 ms	easy	Song <i>et al.</i> (2003)
mixing by micro-plumes		1 μl	1 s	relatively hard	Miyake <i>et al.</i> (1993)
mixing by hydrophobic barriers ^d		1 nl	<1 s	easy	Chen <i>et al.</i> (2003), Yamada & Seki (2003)

^bMixing is achieved by diverting fluids through alternating inlet/outlet channels of stacked sheets. This mixer has also been used for gas flows, with mixing achieved in 30 μs at a gas velocity of 15 m s^{-1} .
^cStream A is oil. Stream B consists of three different aqueous components that are introduced into the oil stream to form immiscible microreactors. The fluids in the microreactors are recirculated, promoting mixing via chaotic advection.
^dMixing by hydrophobic barriers uses a hydrophilic barrier at the end of the channel. Another fluid is then loaded into the main channel. Pressure is increased until the fluid in the side channel wets the hydrophobic barrier and is siphoned into the main channel, where it mixes with the other fluid.

Table 2. *Active micromixers grouped by underlying physical principles*

(The references to literature sources are given in parentheses. The phenomena that have not been tried in real-world devices but are likely to generate good mixing are printed in *italics*. Methods that use chaotic advection are denoted with a star (*).)

with moving parts		
rotary motion	oscillatory motion	without moving parts
magnetic stirring (Lu <i>et al.</i> 2002)	PZT ultrasonic vibration (Zhu & Kim 1998; Yang <i>et al.</i> 2001)	MHD convection* (Bau <i>et al.</i> 2001; Yi <i>et al.</i> 2002)
<i>electrorotation</i>	thermal actuation of a gas bubble (Tsai & Lin 2002)	EHD convection (Choi & Ahn 2000)
	actuation of magnetic microspheres* (Suzuki & Ho 2002)	electrokinetic instability (Oddy <i>et al.</i> 2001)
	microcavity streaming around acoustically driven air bubbles (Liu <i>et al.</i> 2003)	
	<i>magnetic actuation of the droplets of paramagnetic or ferromagnetic liquids</i>	

(b) *Oscillatory motion*

Micromixing systems have been developed that use acoustic waves to generate oscillatory motion, which promotes mixing (Zhu & Kim 1998). Waves were generated by a piezoelectric transducer (PZT) located at the solid–liquid interface at the bottom of the mixing chamber. As these waves propagated through the chamber, they generated vertical and lateral motions throughout the fluid; these motions, in turn, promoted mixing. The transducer itself was fabricated on a silicon wafer through a four-step process. A signal generator generated sinusoidal waves, which were amplified and fed to the transducer. The most effective mixing was observed with resonance frequencies of the thickness-mode vibration of the film. This device had a 2 μl mixing volume.

A similar device has been developed with an oscillating, silicon diaphragm driven by a PZT transducer (Maeda *et al.* 2000). The diaphragm was bonded to a mixing chamber etched out of glass. During continuous operation, the device had a flow rate of 100 $\mu\text{l min}^{-1}$ in a laminar flow regime. When the transducer was operated at a frequency of 48 kHz, it generated ultrasonic vibrations which, the authors claimed, created turbulence in the fluid. Under these conditions, the system became well mixed within 2 s.

A different approach with a nozzle-diffuser micropump actuated by a thermal bubble has been used to create an oscillatory-motion micromixer (Tsai & Lin 2002). The micropump created an oscillatory flow in the direction perpendicular to the interface between the two laminarly flowing fluids. These flows increased the contact area between the fluids and thus promoted effective mixing. The mixing channels were fabricated in a silicon wafer through a deep reactive ion etching process. The channels were 50 μm deep, and the inlet/outlet ports were 500 μm deep. Thermal bubbles were

generated by a heater made of copper wires printed on a glass plate. This plate was bonded to the silicon wafer to seal the device. At a flow rate of $6.5 \mu\text{l min}^{-1}$ and at a pulse frequency of *ca.* 200 Hz, the system achieved effective mixing in *ca.* 1 s over 10 mm of the channel.

Another approach to oscillatory-motion micromixing is based on acoustic microstreaming around an array of small air bubbles resting at the bottom of the mixing chamber (Liu *et al.* 2003). When the bubbles were made to vibrate by a sound field, they created steady circular flows around them. The device was assembled from a deoxyribonucleic acid (DNA) microarray taped to a glass chip having an array of air-bubble traps (i.e. circular wells) milled into its surface. A PZT was glued to the glass plate. When the transducer vibrated at 5 kHz, mixing in the $50 \mu\text{l}$ chamber was achieved within a few seconds. It was demonstrated that a polymerase chain reaction (PCR) performed in this micromixer was more than five times faster than in a conventional, large-scale device.

(c) MHD mixer

An active micromixer has been developed that uses electric and magnetic fields to create Lorentz forces that induced MHD flows in a solution of an electrolyte (Bau *et al.* 2001). The device was fabricated from low-temperature co-fired ceramic tapes. Electrodes were created with gold paste and were placed parallel to the channel. A permanent magnet was placed under the mixing device. The mixing chamber was 1 mm deep, 4.7 mm wide and 22.3 mm long (a volume of *ca.* $100 \mu\text{l}$). When potential difference was applied to the electrodes, Lorentz forces were generated parallel to the axis of the chamber, and the solution was mixed within several seconds.

A more elaborate design using MHD has been developed (Yi *et al.* 2002), reminiscent of the original arrangement of two blinking vortices that Aref (1984) used to demonstrate chaotic advection. The device consisted of a small cylindrical chamber (*ca.* $400 \mu\text{l}$) with an electrode deposited on its side wall. Two additional, copper-wire electrodes were placed eccentrically inside the chamber on the bottom. The chamber was positioned inside a uniform magnetic field parallel to the axis of the cylinder, and mixing was induced by applying a potential difference alternately (with period T) between one of the wire electrodes and the circular side-wall electrode. For large values of T , the flows that developed in the chamber were chaotic (as evidenced by the motions of particle tracers), and effective mixing was achieved within *ca.* 40 cycles.

(d) Electrokinetic instability

This type of micromixing device employs oscillating electro-osmotic flow induced by charge separation at a liquid–solid interface (Oddy *et al.* 2001). Alternating electrical currents created flow instabilities that resulted in rapid stretching and folding of the fluid and thus in effective mixing. Two micromixers were developed: one had channels cast out of PDMS and sealed with a glass slide; the other had channels fabricated from borofloat glass substrates. The first micromixer had platinum microelectrodes that generated electrokinetic instability throughout the entire channel. The second micromixer confined the electrokinetic instability to a small mixing chamber, and achieved effective mixing within 3 s for a flow rate of $0.5 \mu\text{l min}^{-1}$. The time to attain effective mixing was less than 1% of the characteristic diffusion time.

(e) Magnetic microspheres

One such micromixing device had a channel with two conductors embedded below it (Suzuki & Ho 2002). The channel was loaded with magnetic microspheres. When electrical current was applied to the conductors, a magnetic field was created driving the microspheres between the two conductors. The prototype of the device—with a straight channel, two inlets and one outlet—was fabricated via a seven-step process, with the channel walls made out of SU-8 photoresist and coated with polyethylene glycol (PEG), and the electrodes made out of copper; this design was subsequently optimized into a serpentine channel. The authors showed that by using a time-dependent magnetic field, the microspheres could be moved from one electrode to another tracing chaotic paths in the fluid and thus promoting chaotic advection. Numerical simulations indicated that at a flow rate of $40\text{ }\mu\text{m s}^{-1}$, effective mixing occurs within four periods of perturbation (i.e. within *ca.* 4 s in a $160\text{ }\mu\text{m}$ channel).

4. Self-assembly in microfluidics

Based on the short survey of active micromixers in the preceding section, we observe that *efficient* micromixers use either

- (i) high-frequency fields/motions (e.g. rapidly vibrating membranes or rapidly rotating bars) or
- (ii) multiple copies (an array) of mixing elements (e.g. stirrer-bars, vibrating beads, electrodes).

In microfluidic systems, both of these characteristics are desirable: for continuously and rapidly flowing fluids, a single copy of a mixing device might not give rise to efficient mixing. On the other hand, microfabrication of an array of micromixers may be prohibitively complicated, especially in light of their potential commercialization.

In problems where conventional means of microfabrication fail, self-assembly is often a viable alternative. Self-assembly has been successfully used to prepare three-dimensional optoelectronic devices (e.g. photonic crystals (Xia *et al.* 2001)), micro-electronic circuits on curved substrates (Jacobs *et al.* 2002), new types of nano-structured materials (Moriarty 2001), and sensory devices (Krasteva *et al.* 2002); we believe it can also find uses in microfluidics. While organization of static microfluidic architectures would require equilibrium self-assembly, that of microfluidic components with moving parts (e.g. active mixers) would necessitate the use of dynamic self-assembly (DySA): that is, self-assembly in which parts of a system organize and function only when energy is delivered to them externally (Whitesides & Grzybowski 2002; Grzybowski *et al.* 2003). In this work, we used DySA to prepare arrays of highly efficient, rotary micromixers self-assembling in and powered by an external, rotating magnetic field.

5. DySA of rotating, magnetic particles and mixing

The idea behind our current application originates from our earlier work (Grzybowski *et al.* 2000, 2002; Grzybowski & Whitesides 2002*a, b*; Whitesides & Grzybowski 2002) on collections of magnetically doped, polymeric particles rotating at a liquid–air or liquid–liquid interface in a magnetic field of a permanent, rotating bar magnet

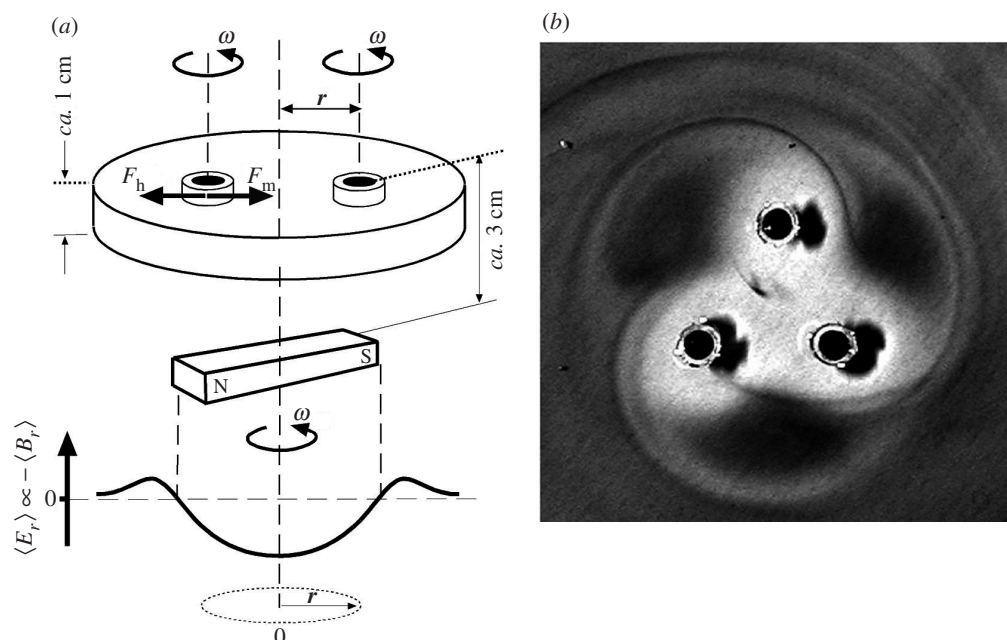


Figure 1. (a) The simplest version of the experimental arrangement used in DySA of magnetic particles. Circular discs (0.1–2 mm in diameter) are usually made by micro transfer moulding (Xia *et al.* 1996) from poly(dimethyl siloxane) (PDMS, Dow Corning) doped with magnetite (15–30% b/w). The discs are placed at a liquid–air interface and are fully immersed in the liquid except for their top surface. A permanent bar magnet (KIKA Labortechnik) of dimensions $L \sim 5.6 \text{ cm} \times W \sim 4 \text{ cm} \times T \sim 1 \text{ cm}$ is placed *ca.* 1–3 cm below the interface and rotated with angular velocity ω (200–1100 RPM). The magnet is magnetized along its longest dimension and has magnetization $M \sim 1000 \text{ G cm}^{-3}$. Magnetic force F_m attracts the discs towards the axis of rotation of the magnet. The spinning discs repel one another by pairwise hydrodynamic forces F_h . The graph below the scheme has the profile of the average radial component of the magnetic induction—proportional to the energy of the magnetic field—in the plane of the interface. The photograph in (b) shows a simple, triangular aggregate formed by three rotating discs.

(figure 1a). The rotating magnet produces an average confining magnetic potential that acts on all particles and results in a force on them directed towards the axis of rotation of the magnet. The rotation of the particles in the fluid gives rise to repulsive, hydrodynamic interactions between them. As a result of the interplay between the magnetic and the hydrodynamic forces, the spinning particles organize into regular structures (figure 1b).

The systems of rotating particles are, in several respects (Grzybowski *et al.* 2002), analogous to assemblies of co-rotating point vortices, which have been extensively studied in the context of mixing. The flowlines around the spinning particles in the plane of an interface to which they are confined are qualitatively similar to those around point vortices (Kuznetsov & Zaslavsky 2000), and—at some locations of the interface and for some ranges of controlling parameters—can give rise to chaotic advection (i.e. to very efficient mixing).

Unlike the point vortices, however, the spinners are finite in the vertical direction, and can thus mix fluids through the Taylor vortices they create above and below the

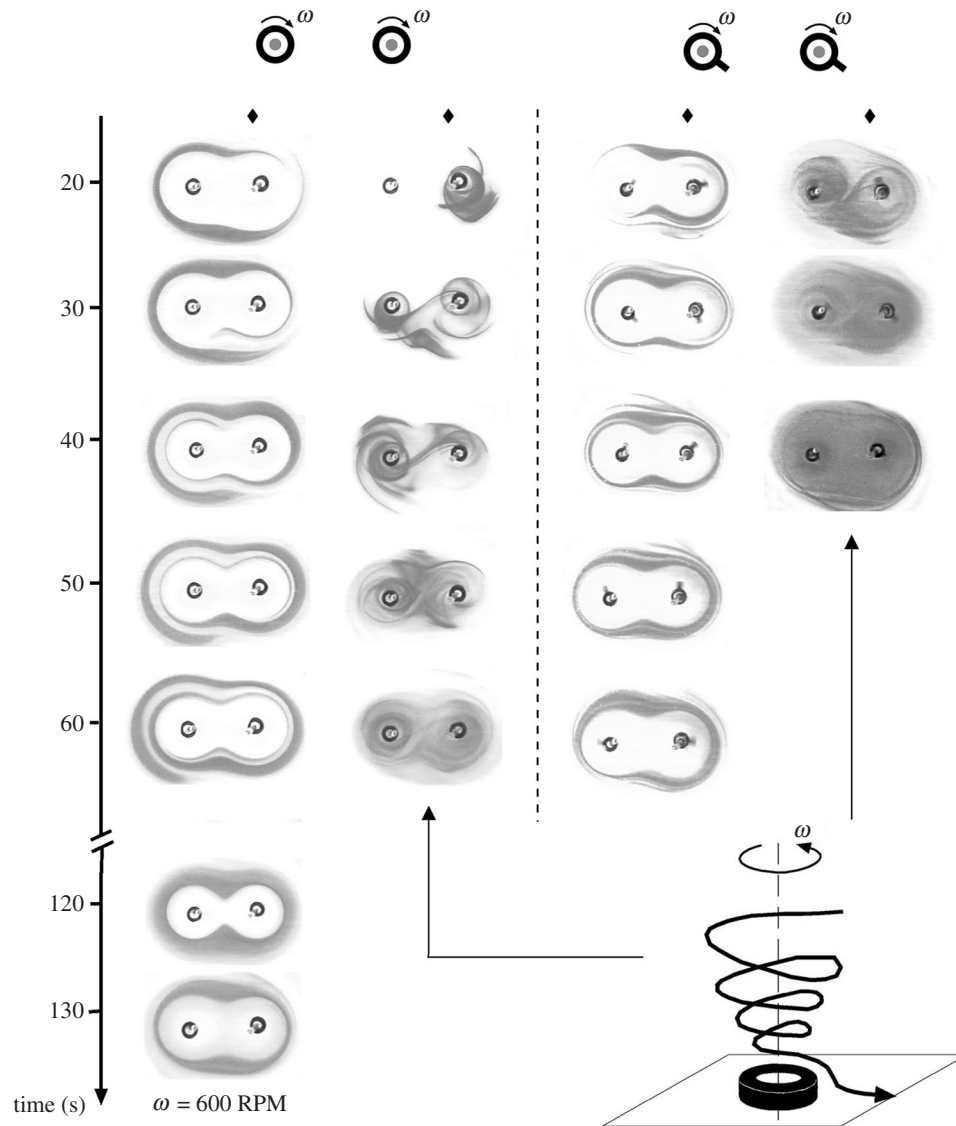


Figure 2. Mixing in systems of two rotating rings. The rings are held in place by thin needles and are rotating at $\omega = 300 \text{ RPM}$ at an interface between perfluorodecalin (PFD) and a 2:1 b/w solution of glycerol and water. Each column shows flowlines around the rings visualized at different times. At time $t = 0$, a small dyed blob of glycerol/water solution is introduced into the glycerol/water layer at a location marked by a diamond. In the first and third columns (from the left) the blob is placed directly at an interface; in the second and fourth columns, it is placed slightly above it. In the latter case, the dyed liquid spirals down onto the spinners, as shown in the inset.

plane of the interface. In fact, this out-of-plane mixing is more efficient than mixing due to the flows within the interfacial plane. Figure 2 shows systems of two magnetic rings rotating at an interface between perfluorodecalin and a 2:1 b/w mixture of glycerol and water; the rings rotate around thin needles held 1 cm apart. In the

first column on the left, a small blob of a dyed glycerol/water solution is introduced directly onto the interface. The flows around the spinners are laminar and the mixing occurs predominantly by diffusion. Also, the dye never enters a high-pressure, 8-shaped region around the spinners. In contrast, when the dyed liquid is introduced above the interface (second column from the left), it rapidly spirals down onto the spinners and then winds around them in complex, three-dimensional paths mixing the coloured liquid efficiently. The efficiency of mixing can be further increased by changing the shape of the spinning particles. For example, rings with small ‘tails’ sweep larger areas of the interface, and can mix fluids more rapidly and over a larger extent. As in the case of circular spinners, mixing is poor in the plane of the interface (third column from the left), and efficient in the bulk of the liquid (the rightmost column).

6. A magnetic micromixer based on DySA

The requirement for the particles to spin at an interface is not practical in microfluidic applications. On the other hand, when the spinners are immersed in the bulk of the liquid, they move towards the poles of the permanent magnet and sediment at the bottom of a container. There, they perform ill-defined motions that often bring them close to one another. Because at short separations the particles interact through strong, attractive forces between the magnetic dipoles induced in them by the external magnetic field, they aggregate into few large assemblies. The increased hydrodynamic drag these assemblies experience causes them to rotate more slowly than the external field. In effect, instead of having an array of rapidly rotating mixing elements, one ends up with just a few slow mixers.

(a) Magnetic flux concentrators

We solved the problem of uncontrolled aggregation of fully immersed magnetic particles by introducing field concentrators above the rotating magnet and thus modifying the profile of the external magnetic field. We prepared arrays of ferromagnetic concentrators 25–100 μm in diameter by micromoulding magnetically doped PDMS (50% b/w) into an array of wells embossed on the surface of a PDMS slab. A stationary permanent magnet of magnetization *ca.* 0.05 T along the vertical direction was positioned directly below the array and on the axis of rotation of the permanent magnet producing the rotating field. This magnet concentrated the magnetic field over the region of the PDMS patterned with concentrators (figure 3a). The concentrators deflected the field lines above the stationary magnet (figure 3b(i)) from the vertical direction, and thus created a field gradient in the plane parallel to the surface of the PDMS. When a ferromagnetic particle was placed above the concentrators, it experienced a horizontal magnetic force. The magnitude of this force was proportional to the derivative of the time average—over one revolution of the rotating magnet—of the horizontal component of magnetic induction $F_{m,x} \propto \partial\langle B_x \rangle / \partial x$, and it was directed towards the centre of each concentrator.

(b) Aggregation of ferromagnetic particles

When a solution containing small ferromagnetic particles (iron filings, *ca.* 5 μm in diameter) was put onto the PDMS surface, the magnetic field polarized the particles and they aggregated above the concentrators into needle-like aggregates (figure 3c).

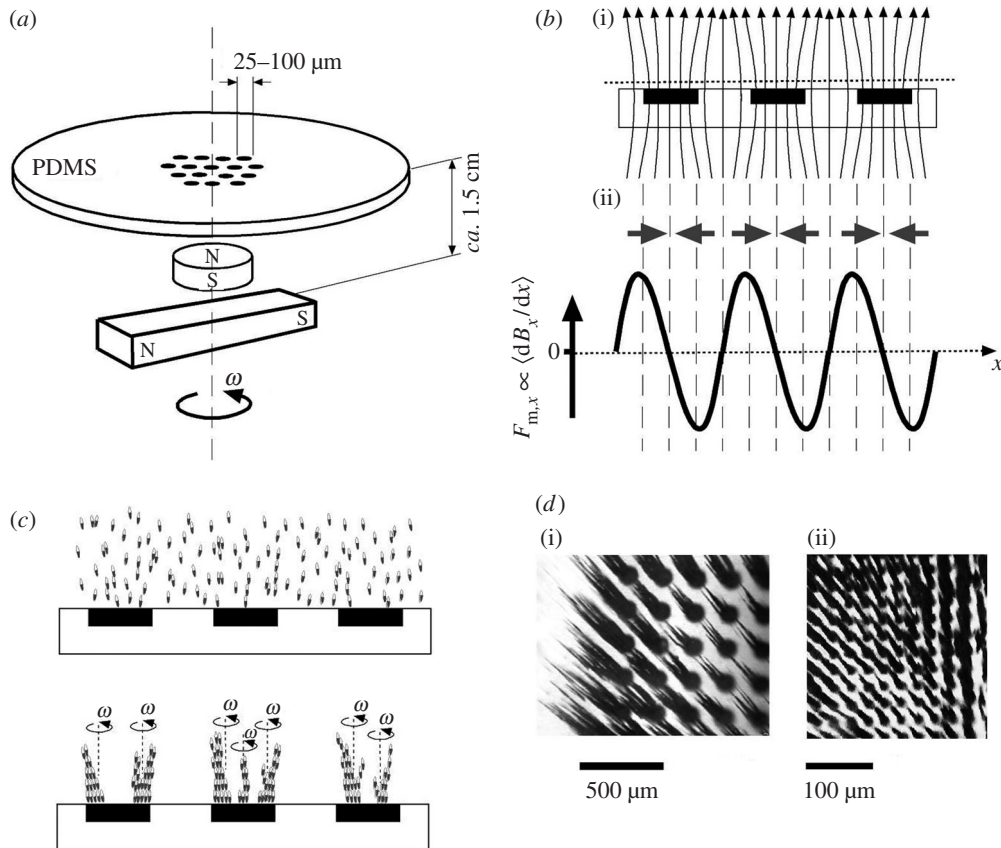


Figure 3. (a) Scheme of the experimental arrangement used to create an array of magnetic micromixers above a patterned PDMS surface. (b) (i) The deflection of the field lines by an array of concentrators. (ii) A corresponding profile of the horizontal magnetic forces $F_{m,r}$ acting in the plane just above the concentrators (dotted line). These forces are directed towards the centres of the individual concentrators. (c) Aggregation of magnetic particles from initially uniform dispersion in the fluid into needle-like aggregates above the concentrators. Each needle rotates with angular velocity ω equal to that of the external rotating magnet. (d) Several needles form over large concentrators (i). Smaller concentrators (less than *ca.* 50 μm) have exactly one, conical needle above each concentrator (ii).

Within each needle, the particles were held together by magnetic dipole–dipole interactions. The needles pointed in the direction of the external magnetic field (approximately, vertical), and rotated around their bases with angular velocity ω equal to that of the external rotating magnet. The number of needles per concentrator was related to its size: large concentrators (greater than 50 μm in diameter) had several needles above them (figure 3*d*(i)), while smaller ones had exactly one cone-shaped needle (figure 3*d*(ii)).

(c) Fabrication of the device

The array of rotating needles self-assembling above the concentrators was the working element of the microfluidic mixer. The device was fabricated as follows. First,

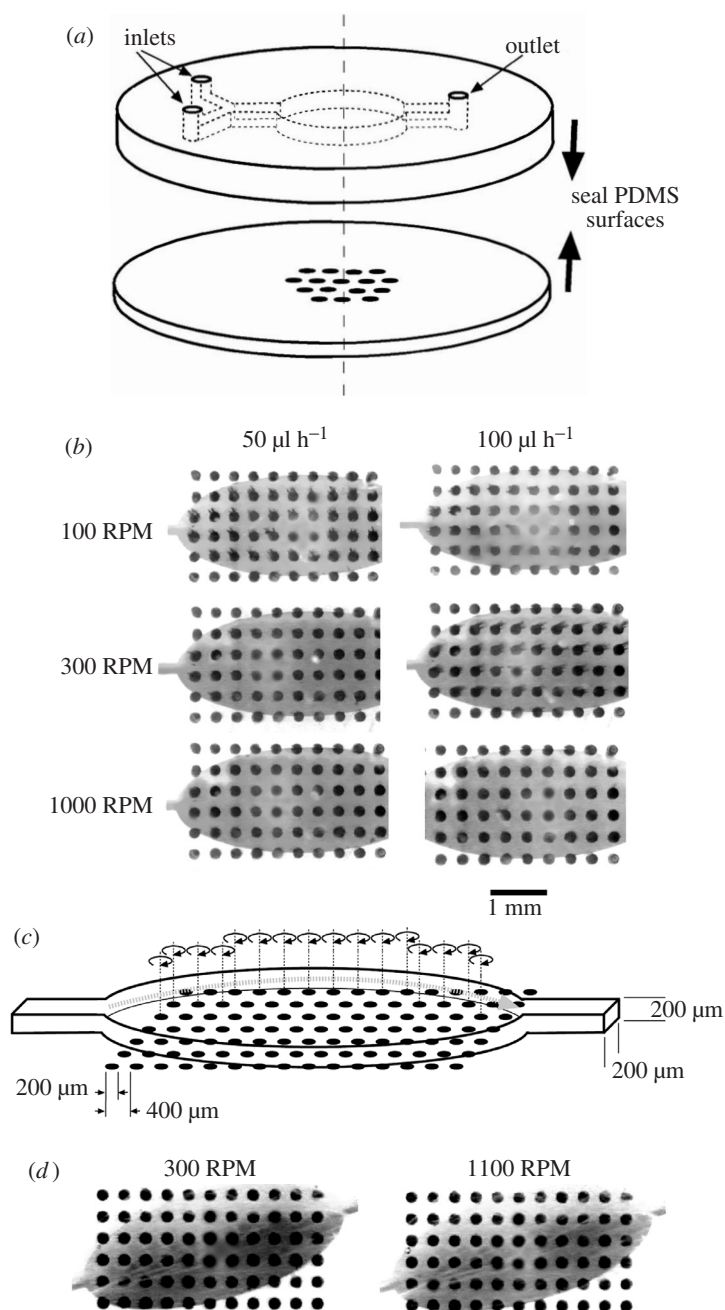


Figure 4. (a) Assembly of the microfluidic mixer. (b) Optical micrographs of mixing in an oval-shaped chamber for different values of rotational speeds and flow rates. The fluid dyed with 'crystal violet' appears grey, while the one dyed with 'acridine yellow' appears white. The scheme in (c) illustrates the streaming effect (inefficient mixing) near the chamber wall where the velocities due to nearby vortices add to the overall flow velocity. (d) Changing the orientation of the chamber with respect to the array of concentrators does eliminate streaming and does not improve mixing. The pictures were taken for a flow velocity of 50 $\mu\text{l h}^{-1}$.

a photolithographic master comprising a positive relief of a 200 μm thick photoresist on a silicon wafer was produced by rapid prototyping (Qin *et al.* 1996). Next, PDMS was cast against this master, cured thermally at 60 $^{\circ}\text{C}$ for 3 h and peeled off to give a PDMS slab with the microfluidic architecture embedded in its surface. Holes were cut in the elastomer using circular punches to form fluid reservoirs. Both the PDMS slab containing the concentrators and that having the microfluidic channels were thoroughly rinsed with water, dried under nitrogen and oxidized in a plasma cleaner for 1 min. They were then brought into conformal contact to seal the device (figure 4a). The assembly was then placed in the rotating magnetic field as described previously (cf. figure 3a).

The liquids were delivered to the inlets from two syringes controlled by a syringe pump. Initially, one syringe filled the device with deionized water, while the other was used to slowly deliver (flow rate $v \sim 5 \mu\text{l h}^{-1}$) a plug of a 1:500 b/w suspension of iron filings in water. As the filings passed over the array of concentrators, they self-assembled into rotating needles. After their self-assembly was complete, the flow rate was increased to 250 $\mu\text{l h}^{-1}$ to remove unbound or weakly bound filings from the mixing chamber.

(d) *Mixing experiments*

Once the device was fully configured, the magnetic field was switched off, and two coloured fluids were flowed laminarly through it. One of the fluids was coloured light violet (with ‘crystal violet’ dye), the other was coloured yellow (with ‘acridine yellow’); both were 1:1 b/v solutions of ethylene glycol (EG) and water (the addition of EG reduced the rate of passive diffusion of the dyes from one liquid to the other). When the magnetic field was turned on, the liquids were mixed. Fluid elements coming onto the array of micromixers were wound around individual micromixers and then transferred onto nearby ones. Experiments with small particle tracers have shown that the paths of tracers initially close to one another usually diverged rapidly (with the exception of the region close to one of the walls; cf. discussion below): some of them travelled to the left of the chamber, some to the right, some were even transported against the overall flow (although this happened infrequently). We observed that the rate of divergence of the trajectories increased with increasing rotational speed ω of the micromixers and decreased with increasing flow rate v . A rigorous quantification of these effects will be a subject of our forthcoming communication.

The efficiency of mixing of two fluids followed the same trends (figure 4b): it increased with increasing ω and decreased with increasing v . Mixing was not complete, however, even for very high rotational speeds and very low flow rates. This effect was caused by streaming of the fluid near the wall where fluid velocities due to nearby vortices were in the same direction as the overall flow (figure 4c). Fluid elements emerging from the inlet channel close to this wall were rapidly transported along the periphery of the mixing chamber and entered the outlet channel virtually unmixed. We tried to minimize this effect by increasing the angle between the inlet channel and the long axis of the array of concentrators so that the liquid would be forced to flow above the central part of the array (figure 4d). Instead, this resulted in nearly laminar flows along the diagonal of the chamber and, consequently, in very inefficient mixing.

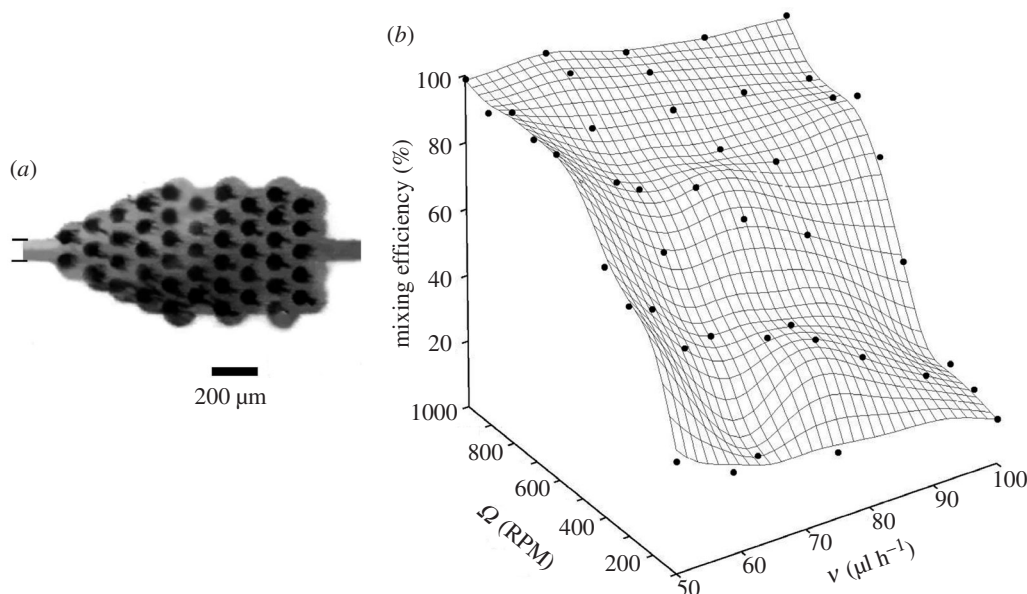


Figure 5. (a) Pear-shaped mixer operating at 700 RPM and at a flow rate of $50 \mu\text{l h}^{-1}$ achieves almost complete mixing. The lines on the right delineate the inlet channel. (b) Mixing efficiency as a function of rotational speed of the magnetic needles and the flow rate.

The streaming effect was eliminated when the mixing chamber had a pear-like shape and its walls had semicircular indentations enclosing the peripheral concentrators of the array (figure 5a). These indentations presented obstacles to the streaming fluid and delaminated it from the walls. The device achieved virtually complete mixing even for high flow rates (figure 5b). The efficiency of mixing was quantified as follows. First, an experimental colour video image was digitized and saved as a bitmap file. An image-analysis program was written in Visual Basic that allowed us to take an RGB intensity profile along a specified line. This line was taken to be the cross-section of the outlet channel. To simplify the analysis, we used clear and blue-coloured solutions of EG and water. We corrected for the red and green components of the video image by dividing the intensity of the blue component by the average of the sum of the green and red components. For laminarly flowing, unmixed fluids, this procedure gave a step function (dark blue/white) across the channel; for fully mixed fluids, it gave a uniform intensity of light blue. For each mixing experiment, we recorded two images: one with the mixers turned off and the fluids flowing laminarly, and the other with mixers working and the fluids mixed. From the first image, we calculated the change in the intensity of blue hue between the channels edges: $\Delta B_{\text{off}} = \langle B \rangle_{\text{right}} - \langle B \rangle_{\text{left}}$, where the terms in angled brackets indicate average intensities taken over the 20 rightmost and the 20 leftmost pixels, respectively. We then calculated a similar quantity, ΔB_{on} from the second picture. Finally, we quantified the mixing efficiency as $\eta = (\Delta B_{\text{off}} - \Delta B_{\text{on}}) / \Delta B_{\text{off}}$. For poorly mixed fluids ($\Delta B_{\text{off}} \sim \Delta B_{\text{on}}$), η was close to zero; for well-mixed fluids it was close to one. Our device gave the values of η close to unity for rotational speeds above 800 RPM and flow rates up to $100 \mu\text{l h}^{-1}$.

7. Conclusions and outlook

Several ingenious designs of both active and passive micromixers have been proposed in recent years. Although the performance of these devices is in many cases satisfactory, their fabrication is usually a tedious, multi-step process. Self-assembly is an alternative, easier approach to making microfluidic components and even systems. The active micromixer described here is an example of an application in which self-assembly significantly simplifies microfabrication and leads to a device with excellent working characteristics.

In a more general context, we envision two types of self-assembly to be useful in microfluidics.

- (i) Templated self-assembly (TeSA) (Wilson *et al.* 2003) can be a strategy for positioning components *within* sealed devices (Kenis *et al.* 1999). It can be of particular value in cases when the components to be placed are not planar (e.g. microspheres, magnetic needles) and/or they need to be organized into three-dimensional structures that are hard to make photolithographically. TeSA can also be helpful in assembling various layers of microfluidic devices and can overcome the problems associated with their precise registration.
- (ii) Dynamic self-assembly (DySA), in turn, can be a basis for reconfigurable/‘smart’ devices controlled by external fields. Such devices could not only be turned on and off, but it could be possible to change their internal structures and/or functions during their operation.

The combination of TeSA and DySA can be a powerful approach to making new types of microfluidic systems.

B.G. gratefully acknowledges financial support from the Camille and Henry Dreyfus New Faculty Awards Program. C.C. was supported in part by the NSF-IGERT program ‘Dynamics of Complex Systems in Science and Engineering’ (DGE-9987577).

References

- Aref, H. 1984 Stirring by chaotic advection. *J. Fluid Mech.* **143**, 1–21.
- Auroux, P., Iossifidis, D., Reyes, D. R. & Manz, A. 2002 Micro total analysis systems. II. Analytical standard operations and applications. *Analyt. Chem.* **74**, 2637–2652.
- Bau, H., Zhong, J. & Yi, M. 2001 A minute magneto hydro dynamic (MHD) mixer. *Sens. Actuat. B* **79**, 207–215.
- Blakebrough, N. 1967 *Biochemical and biological engineering science*. Academic.
- Charrier, J. 1991 *Polymeric materials and processing: plastics, elastomers, and composites*. Oxford University Press.
- Chaté, H., Villiermaux, E. & Chomaz, J. M. 1999 *Mixing: chaos and turbulence*. NATO ASI, Series B, Physics, vol. 373. New York: Kluwer/Plenum.
- Chen, C., Kuo, S., Chu, C. & Teng, F. 2003 A power-free liquid driven method for micro mixing application. In *IEEE Proc. MEMS 2003*, pp. 100–103. Piscataway, NJ: IEEE.
- Choi, J. & Ahn, C. 2000 Active microfluidic mixer for mixing of microparticles and liquids. In *Microfluidic devices and systems*, vol. III, pp. 154–161. Bellingham: The Society of Photo-Optical Instrumentation Engineers.

- Ehrfeld, W., Hartmann, J., Hessel, V., Kiewewalter, S. & Lowe, H. 2000a Microreaction technology for process intensification and high throughput screening. In *Proc. Micro Total Analysis Systems Symp. 2000* (ed. A. van den Berg, W. Olthuis & P. Bergveld), pp. 33–40. Dordrecht: Kluwer.
- Ehrfeld, W., Lowe, H. & Hessel, V. 2000b *Microreactors: new technology for modern chemistry*, 1st edn. Wiley-VCH.
- Evans, J., Liepmann, D. & Pisano, A. P. 1997 Planar laminar mixer. In *IEEE Proc. MEMS 1997*. Piscataway, NJ: IEEE.
- Fogler, H. 1999 *Elements of chemical reaction engineering*, 3rd edn. Englewood Cliffs, NJ: Prentice Hall.
- Grzybowski, B. A. & Whitesides, G. M. 2002a Three-dimensional dynamic self-assembly of spinning magnetic disks: vortex crystals. *J. Phys. Chem. B* **106**, 1188–1194.
- Grzybowski, B. A. & Whitesides, G. M. 2002b Dynamic aggregation of chiral spinners. *Science* **296**, 718–721.
- Grzybowski, B. A., Stone, H. A. & Whitesides, G. M. 2000 Dynamic self-assembly of magnetized, millimeter-sized objects rotating at a liquid–air interface. *Nature* **405**, 1033–1036.
- Grzybowski, B. A., Stone, H. A. & Whitesides, G. M. 2002 Dynamics of self-assembly of magnetized disks rotating at the liquid–air interface. *Proc. Natl Acad. Sci. USA* **99**, 4147–4151.
- Grzybowski, B. A., Wiles, J. A. & Whitesides, G. M. 2003 Dynamic self-assembly of rings of charged metallic spheres. *Phys. Rev. Lett.* **90**, 083903.
- He, B., Burke, B. J., Zhang, X., Zhang, R. & Regnier, F. E. 2001 A picoliter-volume mixer for microfluidic analytical systems. *Analyt. Chem.* **73**, 1942–1947.
- Jacobs, H. O., Tao, A. R., Schwartz, A., Gracias, D. H. & Whitesides, G. M. 2002 Fabrication of a cylindrical display by patterned assembly. *Science* **296**, 323–325.
- Kenis, P. J. A., Ismagilov, R. F. & Whitesides, G. M. 1999 Microfabrication inside capillaries using multiphase laminar flow patterning. *Science* **285**, 83–85.
- Knight, J. 2002 Honey, I shrunk the lab. *Nature* **418**, 474–475.
- Knight, J., Vishwanath, A., Brody, J. P. & Austin, R. H. 1998 Hydrodynamic focusing on a silicon chip: mixing nanoliters in microseconds. *Phys. Rev. Lett.* **80**, 3863–3866.
- Krasteva, N., Besnard, I., Guse, B., Bauer, R. E., Müllen, K., Yasuda, A. & Vossmeier, T. 2002 Self-assembled gold nanoparticle/dendrimer composite films for vapor sensing applications. *Nano Lett.* **2**, 551–555.
- Kuo, K. 1986 *Principles of combustion*. Wiley.
- Kuznetsov, L. & Zaslavsky, G. M. 2000 Passive particle transport in three-vortex flow. *Phys. Rev. E* **61**, 3777–3792.
- Lee, Y. K., Tabling, P., Shih, C. & Ho, C. M. 2000 Characterization of a MEMS-fabricated mixing device. In *ASME Proc. MEMS 2000*, pp. 505–511. New York: ASME.
- Legge, C. 2001 Lab-on-a-chip: scaling down. *Chem. Engineer* **7**, 34–35.
- Liu, R., Lenigk, R., Druyor-Sanchez, R. L., Yang, J. & Grodzinski, P. 2003 Hybridization enhancement using cavitation microstreaming. *Analyt. Chem.* **75**, 1911–1917.
- Lu, L., Ryu, K. & Liu, C. 2002 A magnetic microstirrer and array for microfluidic mixing. *J. MEMS* **11**, 462–469.
- Maeda, R., Yang, Z., Goto, H. & Matsumoto, M., 2000 Active micromixer for microfluidic systems using lead-zirconate-titanate(PZT)-generated ultrasonic vibration. *Electrophoresis* **21**, 116–119.
- Miyake, R., Lammerink, T. S. J., Elwenspoek, M. & Fluitman, J. H. J. 1993 Micro mixer with fast diffusion. In *IEEE Proc. MEMS 1993*. Piscataway, NJ: IEEE.
- Moriarty, P. 2001 Nanostructured materials. *Rep. Prog. Phys.* **64**, 297–381.
- Nguyen, N. & Werely, S. 2002 *Fundamentals and applications of microfluidics*. Boston, MA: Artech House.

- Oddy, M., Santiago, J. & Mikkelsen, J. 2001 Electrokinetic instability micromixing. *Analyt. Chem.* **73**, 5822–5832.
- Ottino, J. 1988 *The kinematics of mixing: stretching, chaos and transport*. Cambridge Texts in Applied Mathematics. Cambridge University Press.
- Plumb, A. 1993 Atmospheric dynamics. Mixing and matching. *Nature* **365**, 489.
- Qin, D., Xia, Y. N. & Whitesides, G. M. 1996 Rapid prototyping of complex structures with feature sizes larger than 20 μm . *Adv. Mater.* **8**, 917.
- Radovanovic, M. 1986 Fluidized bed combustion. In *Proc. Int. Centre Heat Mass Transfer*, vol. 21. Washington, DC: Hemisphere.
- Reyes, D., Iossifidis, D., Auroux, P. A. & Manz, A. 2002 Micro total analysis systems. I. Introduction, theory, and technology. *Analyt. Chem.* **74**, 2623–2636.
- Song, J., Tice, J. D. & Ismagailov, R. F. 2003 Microfluidic system for controlling reaction networks in time. *Angew. Chem. Int. Ed.* **42**, 768–772.
- Stroock, A., Dertinger, S. K. W., Ajdari, A., Mezic, I., Stone, H. A. & Whitesides, G. M. 2002 Chaotic mixer for microchannels. *Science* **295**, 647–651.
- Suzuki, J. & Ho, C. 2002 A magnetic force driven chaotic micro-mixer. In *IEEE Proc. MEMS 2002*, pp. 40–43. Piscataway, NJ: IEEE.
- Tay, F. 2002 *Microfluidics and bioMEMS applications*. Kluwer.
- Tooley, F. 1984 *The handbook of glass manufacture: a book of reference for the plant executive, technologist, and engineer*, 3rd edn. New York: The Glass Industry Division of Ashlee Publishing.
- Tsai, J. & Lin, L. 2002 Active microfluidic mixer and gas bubble filter driven by thermal bubble micropump. In *Transducers 2001—Euroensors XV*, pp. 665–671. Elsevier.
- Walsh, G. 1998 *Biopharmaceuticals: biochemistry and biotechnology*. Wiley.
- West, A. 1984 *Solid state chemistry and its applications*. Wiley.
- Whitesides, G. M. & Grzybowski, B. 2002 Self-assembly at all scales. *Science* **295**, 2418–2421.
- Wilson, J. N., Bangcuvo, C. G., Erdogan, B., Myrick, M. L. & Bunz, U. H. 2003 Nanostructuring of poly(aryleneethynylene)s: formation of nanotowers, nanowires, and nanotubules by templated self-assembly. *Macromolecules* **36**, 1426–1428.
- Xia, Y. N., Kim, E. & Whitesides, G. M. 1996 Micromolding of polymers in capillaries: applications in microfabrication. *Chem. Mater.* **8**, 1558–1567.
- Xia, Y. N., Gates, B. & Li, Y. N. 2001 Self-assembly approaches to three-dimensional photonic crystals. *Adv. Mater.* **13**, 409–413.
- Yamada, M. & Seki, M. 2003 Microfluidic chamber array for generating concentration gradients. In *IEEE Proc. MEMS 2003*. Piscataway, NJ: IEEE.
- Yang, Z., Matsumoto, S., Goto, H., Matsumoto, M. & Maeda, R. 2001 Ultrasonic micromixer for microfluidic systems. *Sens. Actuat. A* **93**, 266–272.
- Yi, M., Qian, S. & Bau, H. 2002 A magneto-hydrodynamic (MHD) chaotic stirrer. *J. Fluid Mech.* **468**, 153–177.
- Zhu, X. & Kim, E. 1998 Microfluidic motion generation with acoustic waves. *Sens. Actuat. A* **66**, 355–360.